Biomass Conversion and Biorefinery (2023) 13:16899–16908
https://doi.org/10.1007/s13399-021-02028-1

ORIGINAL ARTICLE

κ-Carrageenan-based bio-nanocomposite film reinforced with cellulose nanocrystals derived from amla pomace for food packaging

Vidhi Gupta[1] · Rakhi Yadav[1] · Rohit Tanwar[1] · Kirtiraj K. Gaikwad[1]

Received: 15 September 2021 / Revised: 30 September 2021 / Accepted: 7 October 2021 / Published online: 18 October 2021

Abstract
This work reports for the first time the development and characterization of κ-carrageenan-based bio-nanocomposite films incorporated with cellulose nanocrystals (CNC) derived from Indian gooseberry pomace, a major waste from fruits and vegetables processing industry. The CNCs were incorporated in different proportions, viz., 1, 3, 5, and 7%, and solution casting method was used to prepare the films. The effect of CNC loading on the structural, morphological, mechanical, and barrier properties was evaluated. Compared with the control films, CNC-reinforced bio-nanocomposite films showed better barrier and mechanical properties. After 5% CNC loading, water vapor permeability of the films decreased from 3.21 to 2.36 g mm/m^2 day kPa while an increase in the tensile strength from 23.28 to 39.75 MPa was seen. FTIR analysis showed that no structural changes took place in the polymeric matrix after the addition of CNC, while FESEM results showed that higher CNC loadings (7%) lead to agglomeration. Crystallinity of the films increased with the addition of CNC, as evident from XRD. The developed bio-nanocomposite films have the potential to be utilized for high-barrier food packaging applications.

Keywords Cellulose nanocrystals · κ-Carrageenan · Bio-nanocomposite films · Indian gooseberry · Barrier properties

1 1. Introduction

Over the past few decades, considerable research efforts have been devoted to bio-based packaging materials due to growing environmental concerns related to plastics [1, 40, 45]. The worldwide attention to achieve the sustainability agenda of Sustainable Development Goals (SDGs) by 2030 has been the primary driving force for the increasing demand for bio-based polymers in food packaging. Numerous studies have demonstrated the use of biopolymers such as polysaccharides [2], proteins [3], and lipids [4] in the manufacture of biodegradable packaging as they offer many advantages like low cost, renewability, easy availability, and biodegradable nature. However, technological challenges like low tensile strength and poor barrier properties of the biopolymers limit their practical application in the packaging industry [47–49]. To address these challenges, many efforts have been made to tailor the functionalities of these packaging materials. One such approach includes reinforcing the biodegradable polymers with nanofillers by incorporating nanoclays, nanofibers, and nanocrystals [5]. Good barrier properties help to prevent oxidative changes in the food and maintain its quality, while excellent mechanical properties are required to transport and distribute packages in sound condition [41, 42, 46].

Among the broad family of nanofillers, cellulose nanocrystals (CNC), also termed cellulose nanowhiskers, have been widely utilized as the reinforcing nanofillers due to their intriguing properties like large surface area, high aspect ratio, high thermal stability, easy processability, high bending strength, and high Young's modulus [6, 7]. CNCs are extracted from the cellulosic fibers through acid hydrolysis, where amorphous regions get degraded, leading to the release of nanocrystallites [8, 9]. It is well reported in several studies that inclusion of adequate amount of CNCs into the polymer matrix resulted in enhanced mechanical and barrier properties [10–13]. Hence, dispersion of CNCs in the biopolymer matrix could be a practical approach to

✉ Kirtiraj K. Gaikwad
kirtiraj.gaikwad@pt.iitr.ac.in

[1] Department of Paper Technology, Indian Institute of Technology Roorkee, Uttarakhand, Roorkee 247667, India

enhancing the biopolymers' intrinsic properties and broadening their areas of application.

Carrageenans are water-soluble sulfated polysaccharides which are derived from red algae [14]. They consist of linear chains of galactans and can be categorized into three types depending upon the sulfate content: κ (20%), ι (33%), and λ (41%) [15]. κ-Carrageenan (KCGN) extracted from *Kappaphycus alvarezii* seaweed is one of the most popular polysaccharides. It consists of D-galactopyranosyl 4-sulfate and 3,6-anhydro-D-galactopyranosyl moieties with one sulfate group per dimer [16]. It is utilized in various food applications due to its remarkable thickening, stabilizing, and gelling properties [17–19]. Apart from this, the film-forming properties of κ-carrageenan are also well stated. However, these films exhibit low mechanical properties. In order to solve this problem, κ-carrageenan films were blended with nanoclays such as montmorillonite (MMT) and halloysite, which substantially improved the barrier and mechanical properties, yielding films with desirable functions [20–22]. In this context, CNCs could also be promising nanofillers for reinforcing the carrageenan-based films. They could also serve as a potential alternative to the inorganic nanofillers due to their non-abrasive nature, easy processability, and positive ecological footprint [23, 43, 44].

In the current study, it is being hypothesized that the properties of the nanocomposites reinforced with CNCs are strongly dependent not only upon the amount of CNC loading but also on the source of CNC extraction. Therefore, this study aims to develop and characterize κ-carrageenan films incorporated with CNC extracted from the amla (*Phyllanthus emblica)* pomace. The cellulose nanocrystals were added in different proportions, and the films were characterized for their mechanical and water barrier properties. Moreover, the structural and morphological characteristics were also evaluated with the help of FTIR and FESEM studies. The developed nanocomposite films have the potential to be used in food packaging industry for various applications.

2 Materials and methods

2.1 Materials

Food-grade κ-carrageenan was procured from a local shop in Saharanpur, India. Toluene, glacial acetic acid, potassium hydroxide, and sodium chlorite were bought from Himedia Laboratories (India). Methanol, sulfuric acid (98% purity), and glycerol were purchased from Rankem (Avantor Performance Materials, India). All the chemicals mentioned above were utilized without any purification and were of analytical grade. Deionized water was used throughout the experimental procedure.

2.2 Isolation of CNC from amla pomace

CNCs were extracted from amla pomace using the conventional acid treatment method as discussed in our previous study [24]. Briefly, the pomace was subjected to the bleaching treatments (4% w/v sodium chlorite solution containing glacial acetic acid (5%) to maintain the pH around 4) to remove hemicellulose and lignin surrounding the cellulose. This renders chemically purified cellulose fibers. The obtained cellulose was then subjected to acid hydrolysis for 40 min using 64% sulfuric acid. The colloidal suspension of CNC was centrifuged and dialyzed to remove traces of acid. Afterwards, the resulting suspension was freeze-dried and stored till further use.

2.3 Fabrication of KCGN/CNC bio-nanocomposite films

The KCGN/CNC nanocomposite films were developed using the solution casting method, where water was used as the casting solvent. Figure 1 represents the schematic illustration of the fabrication process of k-carrageenan-based bio-nanocomposite film reinforced with different concentrations of cellulose nanocrystals derived from amla pomace. Briefly, cellulose nanocrystals were dispersed in 100 mL of deionized water in different proportions 1, 3, 5, and 7%. The CNC suspension was probe sonicated (SKL-650D, Ningbo Sjia Lab Equipment Co Ltd, China) for 30 min at the frequency of 20–25 kHz to ensure uniform dispersibility of the nanocrystals. To this suspension, κ-carrageenan was added, and subsequently, the film-forming solution (FFS) was heated at 80 °C for 2 h with continuous stirring at 400 rpm to get a homogenous mixture. To this FFS, 37.8% (w/w) glycerol was added with continuous heating for another 40 min. The FFS was then poured into the casting plate and dried at 50 °C in a hot air oven. The dried films were peeled off and stored in controlled conditions (25 °C and 50% relative humidity) until further use. The overall formulation for different films is represented in Table 1. The control sample was KCGN film prepared without the addition of CNC and marked as neat KCGN film.

2.4 Surface color

The surface color of all the films was determined using a Konica Minolta chromameter (Model no. CR-400, Japan). The color of the films was measured using CIE standard D65/10° and expressed in terms of *L*, *a*, and *b* values where *L*, *a*, and *b* depict lightness, redness (+a) -greenness

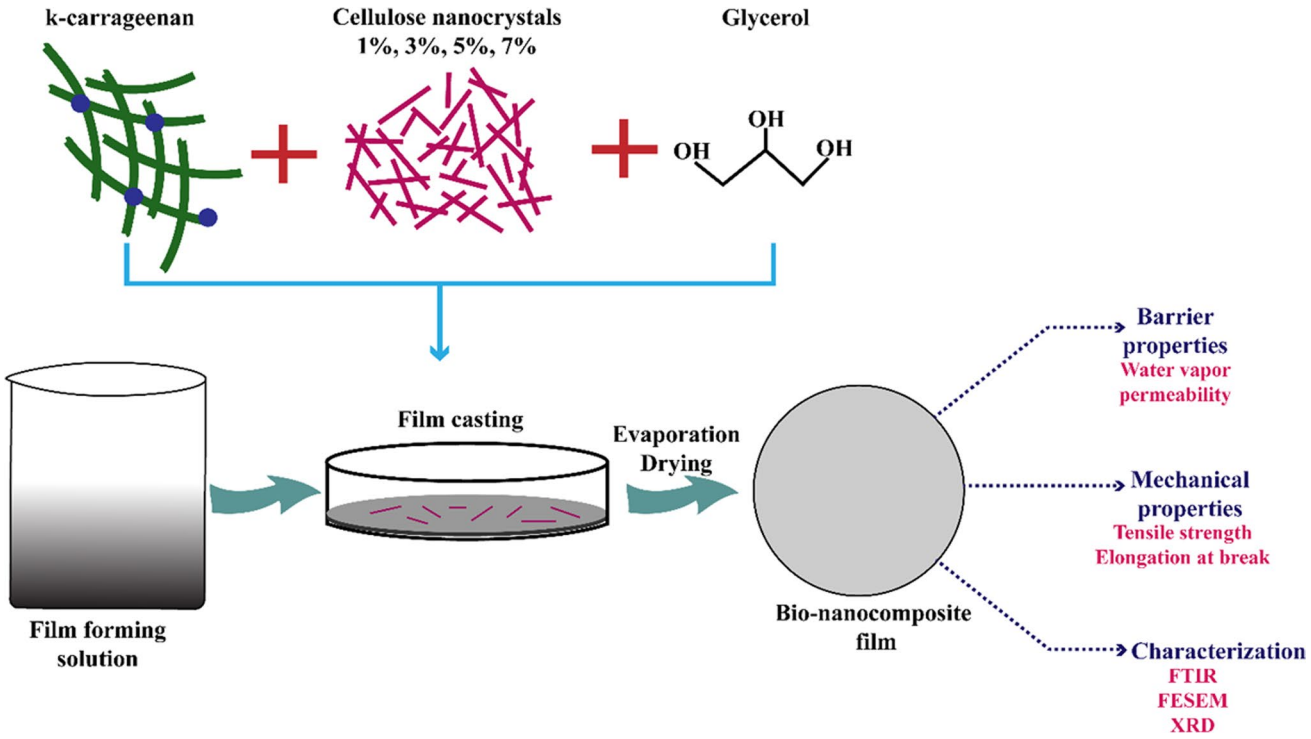

Fig. 1 Schematic illustration of the fabrication process of k-carrageenan-based bio-nanocomposite film reinforced with different concentrations of cellulose nanocrystals derived from amla pomace

Table 1 A typical recipe of the k-carrageenan bio-nanocomposite films containing different concentration of cellulose nanocrystals derived from amla pomace

Sample	Kappa-carrageenan (g)	Cellulose nanocrystals (g)	Total mass (g)
Neat KCGN	2	-	2
KCGN/CNC-1%	1.98	0.02	2
KCGN/CNC-3%	1.94	0.06	2
KCGN/CNC-5%	1.90	0.10	2
KCGN/CNC-7%	1.86	0.14	2

(-a), and yellowness (+b) - blueness (-b), respectively. The color difference value was calculated as per Equation 1.

$$\Delta E = \sqrt{\Delta L^2 + \Delta a^2 + \Delta b^2} \quad (1)$$

where $\Delta L = L_{standard} - L_{film}$, $\Delta a = a_{standard} - a_{film}$, $\Delta b = b_{standard} - b_{film}$

2.5 Mechanical properties

The developed KCGN/CNC films were tested for two mechanical properties, viz., %E (percentage of elongation at break) and TS (tensile strength) using an Instron-3365 Universal Testing Machine (India). The standard procedure described in ASTM D882-02 was used to determine both the properties. A film strip having length and width 10 cm and 1 cm, respectively, was cut for every sample and loaded on the testing machine. The crosshead speed was set at 5 mm/min using a 5-cm primary grip separation. The tensile strength and elongation at break (%) were calculated as the mean value of 5 measurements using Equations 2 and 3.

$$\text{TS (MPa)} = \frac{Maximum\ load\ (N)}{Initial\ cross\ section\ area\ \left(mm^2\right)} \quad (2)$$

$$\%E = \frac{Film\ Extension}{Intial\ length\ of\ sample} \quad (3)$$

2.6 Fourier transform infrared (FTIR)

The interaction between different components of the films was carried out using FT-IR analysis with the help of FT-IR Spectrum Two (Perkin Elmer, USA). The spectra were recorded from 4000 to 400 cm^{-1} wavenumber at 4 cm^{-1} resolution with 4 scans for each sample. All the samples were hot air dried for 24 h at the temperature of 50 °C to remove surface moisture and the spectra was obtained using ATR (attenuated total reflectance) mode.

2.7 Thermo-gravimetric analysis (TGA)

The thermal decomposition behavior of samples was analyzed by using thermo-microbalance (NETZSCN TG209 F3, Wittelsbacherstraße, Germany). Approximately 5 mg of the film sample was taken and heated in the pan at temperature ranging from 25 to 800 °C at a scanning rate of 10 °C/min under a pure nitrogen gas environment flowing 20 mL/min. The weight change was taken as a function of heating temperature.

2.8 Field emission scanning electron microscope (FESEM)

The microstructure of the developed KCGN/CNC films was characterized to study the morphological characteristics of the films at the microscopic level. SEM observations were carried out using a MIRA3 TESCAN field emission scanning electron microscope (USA). All the observations were done under high vacuum conditions using electron beam at an accelerating voltage of 5–10 kV. All the films were firstly gold plated for high-resolution imaging with the help of a sputter coater and then placed over the carbon tape on the aluminum stud. The SEM images were obtained at different magnifications.

2.9 Water vapor permeability (WVP)

The WVTR and WVP of the KCGN/CNC films were calculated using the cup method according to the procedure given in ASTM E-96 method. Before testing, all the films were conditioned in a humidity chamber at 25 °C and 55% relative humidity (RH) for 24 h. Firstly, aluminum cups were filled with 10 g silica gel, and films with the surface area of 25 cm^2 were sealed between the aluminum O ring and the cup. To carry out WVP measurements under controlled conditions, the cups were kept inside a desiccator having 75% RH (NaCl saturated solution). The whole assembly was then placed at 25 °C inside an incubator. The weight of the cups was noted down regularly at a time period of 24 h for 8 consecutive days. The WVTR and WVP of all the KCGN/CNC films were calculated as per Equations 4 and 5, respectively.

$$WVTR\left(g\ day^{-1}mm^{-2}\right) = \frac{\Delta m}{\Delta t\ x\ A} \tag{4}$$

$$WVP\left(g\ mm\ day^{-1}mm^{-2}kPa^{-1}\right) = \frac{WVTR\ x\ X}{\Delta p} \tag{5}$$

where Δm = change in the weight of the films (g), A = area of cross-section (mm^2), X = mean value of film's thickness (mm), Δt = time interval (day), and Δp = water vapor pressure difference above and below the surface of the film (kPa).

2.10 X-ray diffraction analysis (XRD)

An X-ray diffractometer (Rigaku Ultima IV, Japan) operating at 30 mA and 40 kV voltage was used to examine the X-ray diffraction spectra of the developed KCGN/CNC films. The pre-dried film samples were loaded on a quartz plate and then kept inside the sample holder. The XRD patterns of all the films were collected using CuK_α radiation (λ = 1.54 Å) with a scanning speed of 4°/min from 4 to 80°.

2.11 Statistical analysis

Every experimental data obtained in the study was statistically analyzed using SPSS ver.22 (IBM Corporation, USA) to calculate one-way ANOVA (analysis of variance). All the results are shown as the value mean ± standard deviation obtained from the triplicates. The Tukey test ($p < 0.05$) was used at 95% confidence level to test the significant differences.

3 Results and discussion

3.1 Surface color

Film transparency is a critical factor that determines the acceptability of the food product by the consumer as it provides a clear view of the conditions and quality of the food product packed inside it. As presented in Table 2, all the films were found to be transparent without the presence of any color tint. The addition of CNC had a significant effect on the color values of the developed bio-nanocomposite

Table 2 Color values of k-carrageenan bio-nanocomposite films containing different concentrations of cellulose nanocrystals derived from amla pomace

Sample code	*L*	*a*	*b*	ΔE
Neat KCGN	32.04 ± 0.04^{a}	-0.17 ± 0.01^{c}	-0.06 ± 0.01^{b}	64.67 ± 0.01^{e}
KCGN/CNC-1%	33.38 ± 0.03^{c}	-0.17 ± 0.01^{bc}	0.18 ± 0.01^{d}	63.35 ± 0.03^{c}
KCGN/CNC-3%	32.20 ± 0.03^{b}	-0.10 ± 0.01^{d}	0.01 ± 0.01^{c}	64.50 ± 0.02^{d}
KCGN/CNC-5%	36.75 ± 0.02^{d}	-0.37 ± 0.02^{a}	0.33 ± 0.02^{e}	59.88 ± 0.03^{b}
KCGN/CNC-7%	40.34 ± 0.03^{e}	-0.20 ± 0.01^{b}	-0.12 ± 0.02^{a}	56.35 ± 0.03^{a}

films ($p < 0.05$). The lightness, L, value increased significantly from 32.04 for the control film to 40.34 for the film consisting of 7% CNC. The increase in the CNC loading might have increased the reflection from the film surface leading to increasing value of lightness [10]. The *a* value which is representative of redness/greenness was negative for all the films and changed slightly with the varying proportions of the cellulose nanocrystals. The *b* value which expresses yellow-blue color component was also increased.

3.2 Mechanical properties

In order to assess the performance of a packaging material in the real environment, it becomes critical to evaluate its tensile strength (TS) and elongation at break (%EB). Figure 2 shows the TS and %EB of all the KCGN/CNC films, respectively. The TS and %EB of the neat KCGN film were found to be 23 MPa and 4.65%, respectively. After the addition of cellulose nanocrystals, significant changes were observed in the TS and %EB values ($p < 0.05$). As the amount of CNC was increased from 1 to 5%, a considerable increase in the tensile strength of the bio-nanocomposite films was seen as compared to that of neat films. An increase of 68% observed in the tensile strength was seen when 5% CNC was added to the matrix. The increase in the mechanical properties of the films could be probably due to the physical interaction between nanofiller (CNC) and matrix (κ-carrageenan). At higher concentration of CNC loading (7%), tensile strength decreased from 39.02 to the value of 26.66 MPa. The agglomeration of CNCs due to interfacial hydrogen bonding leading to the reduction in the interaction between CNC and polymer matrix could be the rationale for this decreasing trend. However, the TS of KCGN/CNC-7% film was found to be higher than the control KCGN film indicating the effective reinforcing effect of the CNC. The results obtained in our study are similar to that of [25] who reported a 24% increment in the tensile strength of the chitosan films incorporated with 5% cellulose nanocrystals.

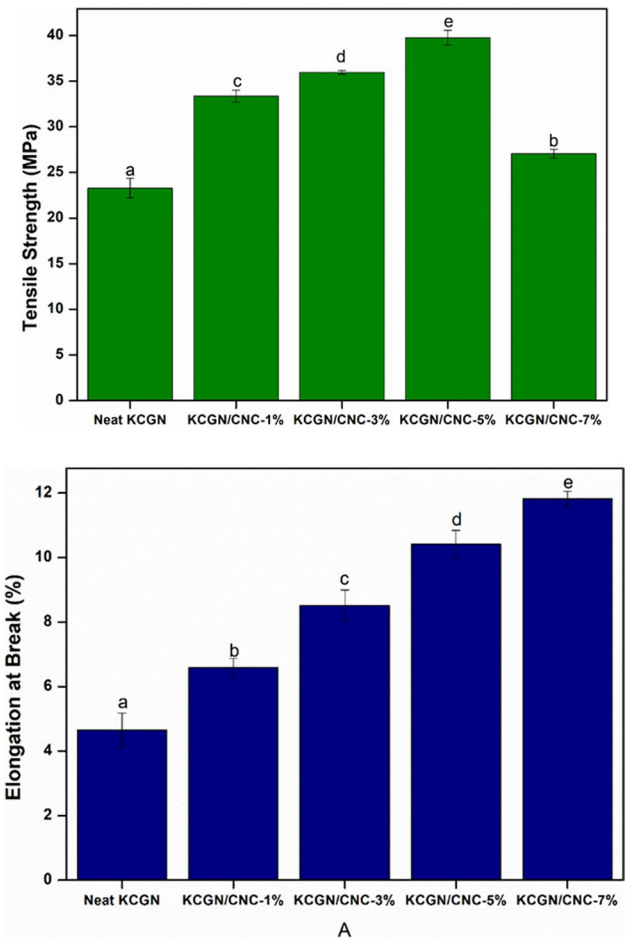

Fig. 2 Tensile strength and elongation at break of k-carrageenan-based bio-nanocomposite film reinforced with different concentrations of cellulose nanocrystals derived from amla pomace

Simultaneously, elongation at break (%EB) was also determined to examine the flexibility of the films. As seen from Figure 2, the value of %EB was found to be proportionally dependent upon the amount of CNC added to the films. Overall, the %EB was seen to be increased considerably with an increase in the CNC from 1 to 7%. The neat film showed elongation at break of 4.16%. Incorporation of 3% and 5% of cellulose nanocrystals increased the %EB to 8.84% and 10.45%, respectively. Although many literature studies such as [26, 27] have reported negative effect of CNC on the values of %EB, however, in our study, it was observed that incorporation of CNCs significantly improved %EB values of the developed bio-nanocomposite films. The increment in the %EB could be attributed due to the good interaction between CNC and κ-carrageenan which resulted in effective transfer of stress through the matrix and CNC layers [28]. These results suggest that the κ-carrageenan films reinforced with cellulose nanocrystals were mechanically stronger than the neat films.

3.3 Fourier transform infrared

The possible chemical interactions between KCGN and CNC were studied with the help of FTIR as shown in Figure 3. All the film samples exhibited a broad peak at around 3337 cm^{-1} which corresponds to the O-H stretching vibration and intramolecular and intermolecular hydrogen bonding [25]. After the addition of CNC into the κ-carrageenan, this peak shifted from 3337 cm^{-1} (neat KCGN film) to a higher wavenumber 3360 cm^{-1} (KCGN/CNC-7%) possibly due to increase in the hydrogen bonds. This indicates interaction between κ-carrageenan and CNC through hydrogen bonding lead to good miscibility between them. Additionally, a relatively small peak at 2940 cm^{-1} related to the of vibration

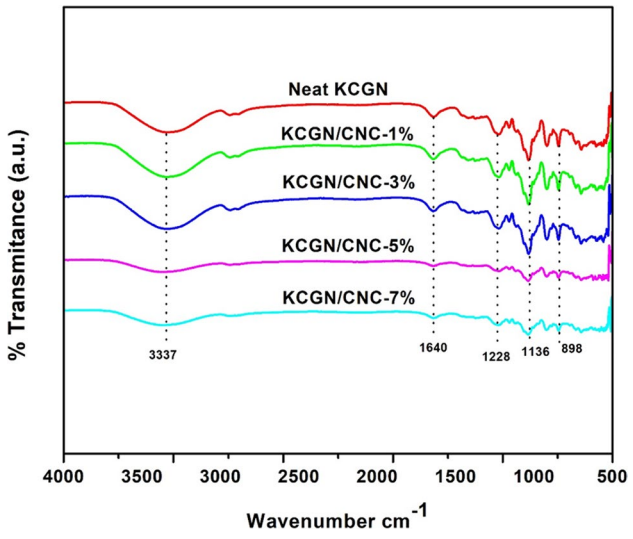

Fig. 3 Fourier-transform infrared spectrum of k-carrageenan-based bio-nanocomposite film reinforced with different concentrations of cellulose nanocrystals derived from amla pomace

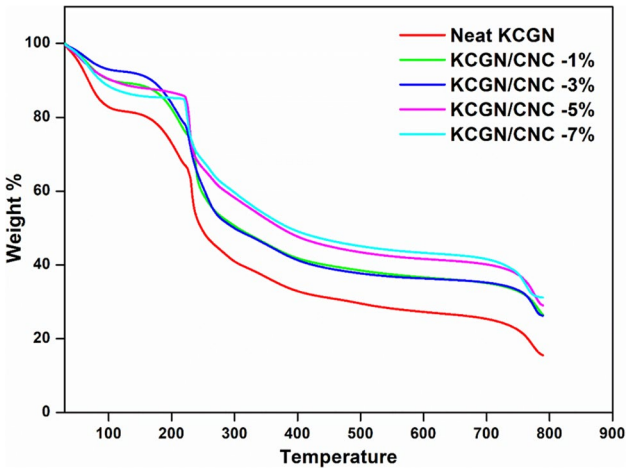

Fig. 4 Thermogravimetric analysis of k-carrageenan-based bio-nanocomposite film reinforced with different concentrations of cellulose nanocrystals derived from amla pomace

of CH groups stretching [29] was also observed and it disappeared almost completely at CNC loading more than 3%. On comparing the FTIR spectrum of the KCGN/CNC film with that of pure film, no new peaks appeared in the films after incorporation of cellulose nanocrystals demonstrating that no chemical reaction takes place between κ-carrageenan and CNC during film formation. In addition to this, a weak peak at 1640cm^{-1} present in all the spectra is representative of the O-H bending of the absorbed water molecules [30]. The peak at 1228 cm^{-1} observed in the spectra of all the films is associated with the ester sulfate group (O═S═O) present in κ-carrageenan [31]. The bands at 1158 cm^{-1} and 1036 cm^{-1} could be associated with C-O and C-C groups stretching vibrations, respectively [32]. Additionally, the peaks at 1113cm^{-1} and 898cm^{-1} observed in all the films corresponds to the vibration of C-O-C and C-H bonds, respectively, present in β-D-glucopyranose units while the peak observed at 843 cm^{-1} is related to O-SO_3 of galactose-4-sulfate [33]. In general, after the loading of cellulose nanocrystals (derived from amla pomace) to the κ-carrageenan polymeric matrix, there were no significant changes in the functional groups of all the KCGN/CNC films, suggesting that the structure of κ-carrageenan was not altered after the incorporation of cellulose nanocrystals.

3.4 Thermogravimetric analysis

Thermal degradation of the neat KCGN and KCGN/CNC bio-nanocomposite films containing cellulose nanocrystals was studied in order to determine the thermal stability of the bio-nanocomposite films. This provides an insight into thermal properties of the developed films and information regarding the processing temperatures during film manufacture. As illustrated in Figure 4, it was seen that all the films were characterized by three regions of thermal decomposition. The region of first degradation was seen in the temperature range of 37 °C to 200 °C due to evaporation of water molecules, while the second region resulted from the depolymerization and dehydration of the polymers between the temperature range of 200 to 400 °C [34]. Finally, the third region of weight loss occurred at temperature above 400 °C due to decomposition of the polymeric matrix. The neat films showed a weight loss of 73.2% in the first region. Upon addition of cellulose nanocrystals, the thermal stability of the KCGN/CNC films increased, where the lowest thermal stability was seen in neat KCGN films. For the films containing 5% and 7% cellulose nanocrystals, the decomposition temperature increased by 20 °C, suggesting that the thermal stability of the films increased after the addition of CNCs. The formation of strong interfacial bonds between the sulfate groups of CNCs and κ-carrageenan might have led to the increase in the onset temperature and hence increased the thermal stability of the films. Moreover, the presence of CNC in the crystallite form could also be a possible rationale for the improvement of the thermal stability of bio-nanocomposite films. After the end of the heating cycle, the residue left was found to be 15.7%, 26.2% 26.6%, 29%, and 31.3% for KCGN, KCGN/CNC-1%, KCGN/CNC-3%, KCGN/CNC-5%, and KCGN/CNC-7% films, respectively.

3.5 Field emission scanning electron microscope

The microstructure of the neat carrageenan film and bio-nanocomposite films is shown in Figure 5. All the films exhibited a smooth and compact structure depicting the

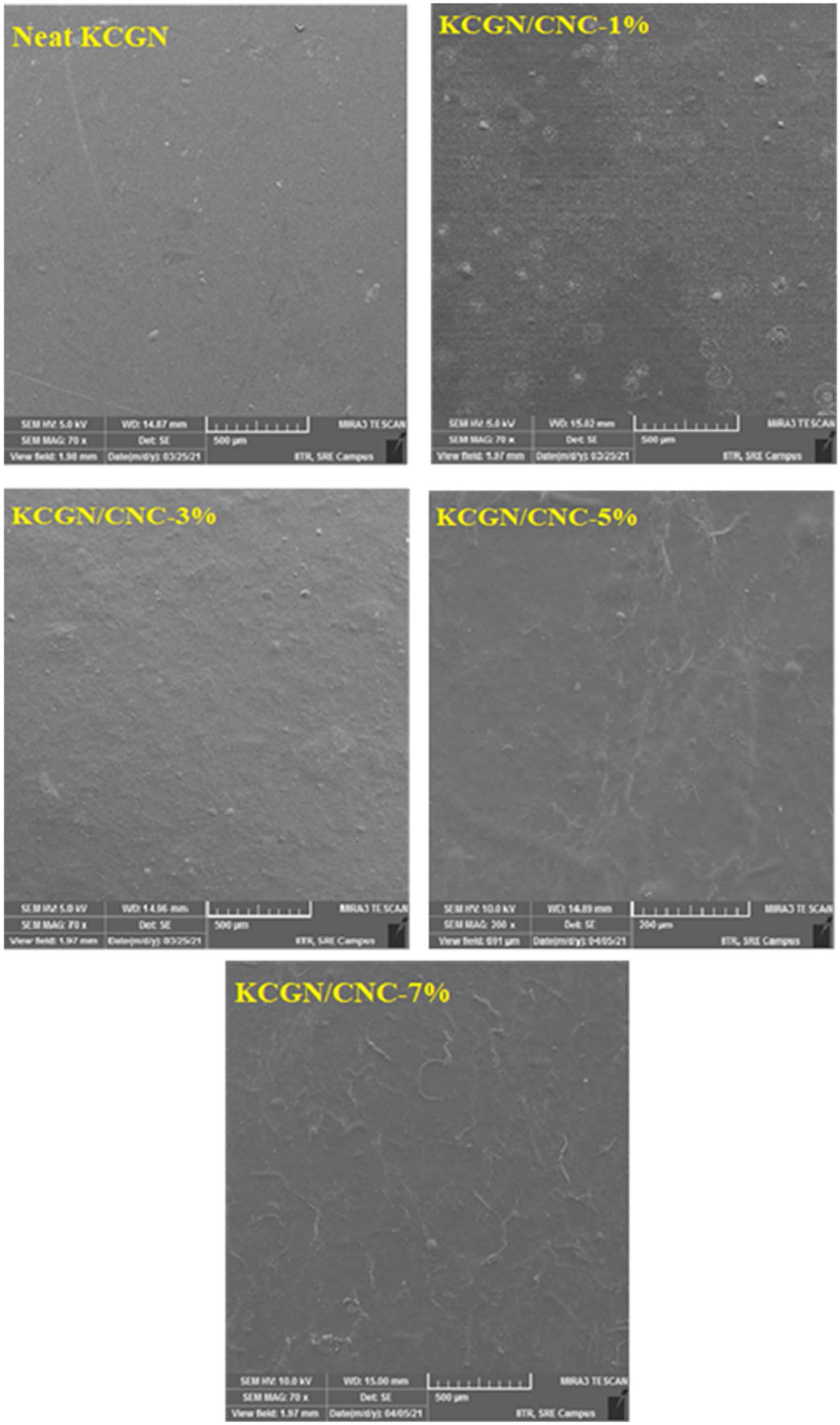

Fig. 5 Scanning electron microscopic images of k-carrageenan-based bio-nanocomposite film reinforced with different concentrations of cellulose nanocrystals derived from amla pomace

homogenous integrity between the different components of the film. From the FESEM images, it can be observed that there are no significant changes in the morphology of neat carrageenan film and bio-nanocomposite films except the fact that nanocomposite films showed the presence of some white spots on their surface. The presence of these white spots could be attributed due to the introduction of cellulose nanocrystals into the polymer matrix. A similar kind of observation was made by Wang et al. [35] who developed carrageenan-based films reinforced with silver nanoparticles. Addition of CNC up to 5% did not affect the microstructure adversely and no cracks and bubbles were observed. The surface of the films was homogenous and no phase separation was seen, indicating good interfacial adhesion between κ-carrageenan and CNC. The nanocomposite films KCGN/CNC-3% and KCGN/CNC-5% showed a dense and compact structure. It is likely that the CNCs were dispersed efficiently into the matrix. Contrary to this, addition of 7% CNC resulted in slightly rough surface of the films, possibly due to the agglomeration of nanocrystals. At higher concentrations, CNCs tend to self-assemble due to strong intermolecular bonds between the surface hydroxyl groups. This agglomerated phenomenon gave rise to the formation of ridges as observed in the SEM image of KCGN/CNC-7% nanocomposite film. Similar results were reported by Doh et al. [36] where alginate films incorporated with 10% cellulose nanocrystals from brown seaweed showed agglomerated surface.

3.6 Water vapor permeability

The WVP of the developed films is depicted in Figure 6. The water vapor permeability of neat KCGN films without CNC was found to be 3.21 g mm/m^2 day kPa, and the water vapor barrier properties of the nanocomposite films was significantly influenced ($p < 0.05$) by the addition of cellulose nanocrystals derived from amla pomace. Upon blending the κ-carrageenan with CNCs, the WVP of the films was found to be decreasing exponentially with the increase in CNC content. The WVP of KCGN bio-nanocomposite films decreased from 3.21 to 2.25 g mm/m^2 day kPa as the concentration of CNC was increased from 1 to 7%. The KCGN/CNC-7% exhibited the highest water barrier properties. The enhancement in the water barrier properties of the KCGN/CNC could be possibly due to uniform dispersion of CNCs throughout the matrix. The dispersed CNC acted as a nanofiller, inducing the tortuous pathway to the water vapor and thereby hindering the diffusion of water molecules through the matrix. On the other hand, in case of the neat KCGN film, there is no physical barrier to the water so it can permeate through the polymer matrix easily. As a result of which the water vapor permeability was seen to be highest in the neat film (approximately 3.21 g mm/m^2 day kPa). These

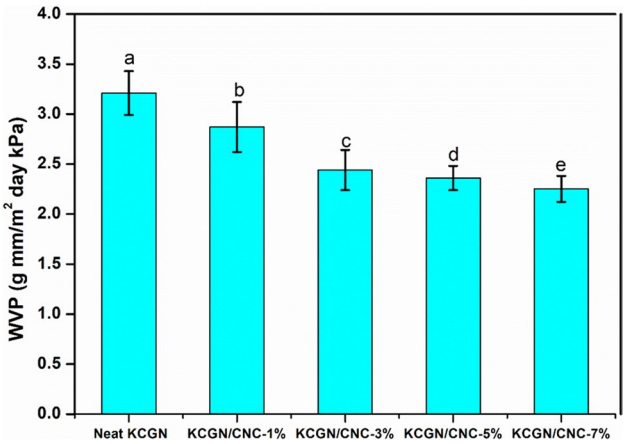

Fig. 6 Water vapor permeability of k-carrageenan-based bio-nanocomposite film reinforced with different concentrations of cellulose nanocrystals derived from amla pomace

results in the present study are in agreement with Oun et al. [37] who reported a similar decreasing pattern in the WVP of carboxymethyl cellulose (CMC) films incorporated with cellulose nanocrystals derived from wheat, rice and barley straw. Kassab et al. [38] also reported improvement in water barrier properties of κ-carrageenan-based films containing CNC from sugarcane bagasse. Our results indicate that the water barrier properties of the κ-carrageenan (KCGN/CNC) bio-nanocomposite films improved significantly when reinforced with CNCs derived from Indian gooseberry pomace and these films could be utilized for packaging applications of different moisture sensitive foods.

3.7 X-ray diffraction analysis

The XRD analysis of the KCGN/CNC films was carried out to evaluate the crystalline nature of the films and effect of addition of CNC on the crystallinity as crystallinity plays a vital role in determining the mechanical properties. Figure 7 depicts the X-ray diffractograms of the neat film (KCGN) and the films incorporated with different contents of cellulose nanocrystals (KCGN/CNC-1%, KCGN/CNC-3%, KCGN/CNC-5%, and 7%). The KCGN and KCGN/CNC-1% film exhibited a characteristic peak at $2\theta = 20.4°$ indicating that the addition of low content of CNC does not have any significant effect on the crystalline nature of the films. However, at higher loadings of CNC, the intensity of this peak increased and got shifted to a higher angle ($2\theta = 21.46°$ and 22.2° for 3% and 5% CNC loading, respectively). KCGN/CNC-5% films showed peaks at $2\theta = 22.2°$, 29°, and 41.18°, while the peaks at $2\theta = 21.41°$, 27.82°, 28.91°, and 40.91° were observed in the bio-nanocomposite film with 7% CNC loading. These peaks are typical of cellulose-I structure and were observed at higher concentration

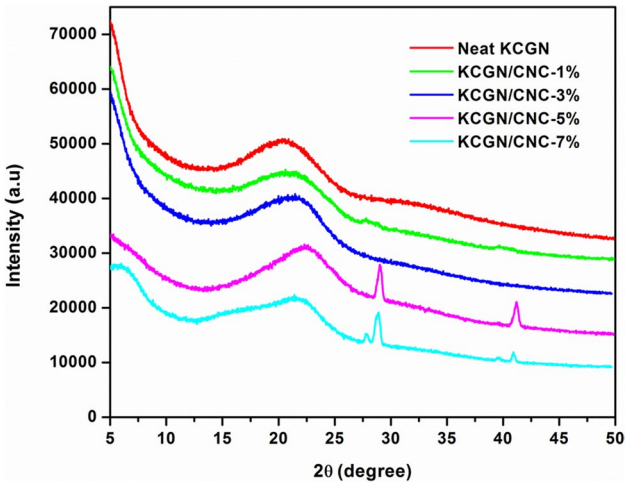

Fig. 7 X-ray diffraction patterns of k-carrageenan-based bio-nanocomposite film reinforced with different concentrations of cellulose nanocrystals derived from amla pomace

of cellulose nanocrystals [39]. A sharp peak at $2\theta = 29°$ was observed in the diffractograms of KCGN/CNC-5% and KCGN/CNC-7% which was absent in other films. This suggests that these films exhibited more crystalline behavior due to more percentage of cellulose nanocrystals.

4 Conclusion

Bio-nanocomposite films based on κ-carrageenan reinforced with cellulose nanocrystals from Indian gooseberry pomace were fabricated for the first time. In this work, it was observed that addition of cellulose nanocrystals significantly improved the tensile strength and barrier properties of the KCGN/CNC films. The improved barrier properties might be due to the tortuous pathways induced after the incorporation of cellulose nanocrystals. FTIR results showed that no structural changes took place in the matrix, while FESEM analysis depicted that no significant morphological changes were seen after addition of CNC. Moreover, it was also revealed that the incorporation of cellulose nanocrystals improved the thermal stability of the developed films significantly. Based on our results, it can be concluded that the CNC-reinforced κ-carrageenan bio-nanocomposite film can open new opportunities for different applications in food packaging. The developed films could be utilized as an effective barrier packaging material in multilayer laminated to protect moisture sensitive products.

Acknowledgment Author K. K. Gaikwad would like to sincerely thank the Department of Science and Technology (DST), Government of India, for the financial support provided under DST INSPIRE Faculty (DST/INSPIRE/04/2018/002544).

Declarations

Conflict of interest The authors declare that there are no conflicts of interest.

References

1. Kumar A, Gupta V, Gaikwad KK (2021) Microfibrillated cellulose from pine cone: extraction, properties, and characterization. Biomass Convers Biorefinery 1–8. https://doi.org/10.1007/s13399-021-01794-2
2. Cazón P, Velazquez G, Ram\'\irez JA, Vázquez M (2017) Polysaccharide-based films and coatings for food packaging: a review. Food Hydrocoll 68:136–148
3. Calva-Estrada SJ, Jiménez-Fernández M, Lugo-Cervantes E (2019) Protein-based films: advances in the development of biomaterials applicable to food packaging. Food Eng Rev 11:78–92
4. Mohamed SAA, El-Sakhawy M, El-Sakhawy MA-M (2020) Polysaccharides, protein and lipid-based natural edible films in food packaging: a review. Carbohydr Polym 238:116178
5. Sanchez-Garcia MD, Lopez-Rubio A, Lagaron JM (2010) Natural micro and nanobiocomposites with enhanced barrier properties and novel functionalities for food biopackaging applications. Trends Food Sci & Technol 21:528–536
6. Grishkewich N, Mohammed N, Tang J, Tam KC (2017) Recent advances in the application of cellulose nanocrystals. Curr Opin Colloid \& Interface Sci 29:32–45
7. Šturcová A, Davies GR, Eichhorn SJ (2005) Elastic modulus and stress-transfer properties of tunicate cellulose whiskers. Biomacromolecules 6:1055–1061
8. Mariano M, El Kissi N, Dufresne A (2014) Cellulose nanocrystals and related nanocomposites: Review of some properties and challenges. J Polym Sci Part B Polym Phys 52:791–806
9. Singh S, Gaikwad KK, Park S-I, Lee YS (2017) Microwave-assisted step reduced extraction of seaweed (Gelidiella aceroso) cellulose nanocrystals. Int J Biol Macromol 99:506–510
10. El Miri N, Abdelouahdi K, Barakat A et al (2015) Bio-nanocomposite films reinforced with cellulose nanocrystals: rheology of film-forming solutions, transparency, water vapor barrier and tensile properties of films. Carbohydr Polym 129:156–167
11. Singh S, Gaikwad KK, Lee YS (2018) Antimicrobial and antioxidant properties of polyvinyl alcohol bio composite films containing seaweed extracted cellulose nano-crystal and basil leaves extract. Int J Biol Macromol 107:1879–1887
12. Perumal AB, Sellamuthu PS, Nambiar RB, Sadiku ER (2018) Development of polyvinyl alcohol/chitosan bio-nanocomposite films reinforced with cellulose nanocrystals isolated from rice straw. Appl Surf Sci 449:591–602
13. Li H, Shi H, He Y et al (2020) Preparation and characterization of carboxymethyl cellulose-based composite films reinforced by cellulose nanocrystals derived from pea hull waste for food packaging applications. Int J Biol Macromol 164:4104–4112
14. Tecante A, del Santiago MCN (2012) Solution properties of $κ$-carrageenan and its interaction with other polysaccharides in aqueous media. Rheology 1:241–264
15. Necas J, Bartosikova L (2013) Carrageenan: a review. Vet Med (Praha) 58
16. Rhein-Knudsen N, Meyer AS (2021) Chemistry, gelation, and enzymatic modification of seaweed food hydrocolloids. Trends Food Sci \& Technol
17. Piculell L (2006) Gelling carrageenans. Food polysaccharides their Appl 239

18. Blakemore WR, Harpell AR, others (2010) Carrageenan. Food stabilisers, Thick gelling agents:73–94
19. Al-Baarri AN, Legowo AM, Rizqiati H, et al (2018) Application of iota and kappa carrageenans to traditional several food using modified cassava flour. In: IOP Conference Series: Earth and Environmental Science. p 12056
20. Nouri A, Yaraki MT, Ghorbanpour M, Wang S (2018) Biodegradable κ-carrageenan/nanoclay nanocomposite films containing Rosmarinus officinalis L. extract for improved strength and antibacterial performance. Int J Biol Macromol 115:227–235
21. Shojaee-Aliabadi S, Mohammadifar MA, Hosseini H et al (2014) Characterization of nanobiocomposite kappa-carrageenan film with Zataria multiflora essential oil and nanoclay. Int J Biol Macromol 69:282–289
22. Wahab IF, Abd Razak SI (2016) Bionanocomposite fim of kappa-carrageenan/nanotube clay: growth of hydroxyl apatite and model drug release. Dig J Nanomater Biostruct 11:963–972
23. Popescu M-C, Dogaru B-I, Sun D et al (2019) Structural and sorption properties of bio-nanocomposite films based on κ-carrageenan and cellulose nanocrystals. Int J Biol Macromol 135:462–471
24. Gupta V, Ramakanth D, Verma C et al (2021) Isolation and characterization of cellulose nanocrystals from amla (*Phyllanthus emblica*) pomace. Biomass Convers Biorefinery:1–12. https://doi.org/10.1007/s13399-021-01852-9
25. Khan A, Khan RA, Salmieri S et al (2012) Mechanical and barrier properties of nanocrystalline cellulose reinforced chitosan based nanocomposite films. Carbohydr Polym 90:1601–1608
26. Slavutsky AM, Bertuzzi MA (2014) Water barrier properties of starch films reinforced with cellulose nanocrystals obtained from sugarcane bagasse. Carbohydr Polym 110:53–61
27. Azeredo HMC, Mattoso LHC, Avena-Bustillos RJ et al (2010) Nanocellulose reinforced chitosan composite films as affected by nanofiller loading and plasticizer content. J Food Sci 75:N1–N7
28. Chaichi M, Hashemi M, Badii F, Mohammadi A (2017) Preparation and characterization of a novel bionanocomposite edible film based on pectin and crystalline nanocellulose. Carbohydr Polym 157:167–175
29. Reddy KO, Guduri BR, Rajulu AV (2009) Structural characterization and tensile properties of borassus fruit fibers. J Appl Polym Sci 114:603–611
30. Haafiz MKM, Hassan A, Zakaria Z, Inuwa IM (2014) Isolation and characterization of cellulose nanowhiskers from oil palm biomass microcrystalline cellulose. Carbohydr Polym 103:119–125
31. cSen M, Erboz EN (2010) Determination of critical gelation conditions of κ-carrageenan by viscosimetric and FT-IR analyses. Food Res Int 43:1361–1364
32. Mujtaba M, Salaberria AM, Andres MA et al (2017) Utilization of flax (Linum usitatissimum) cellulose nanocrystals as reinforcing material for chitosan films. Int J Biol Macromol 104:944–952
33. Distantina S, Fahrurrozi M, others (2013) Synthesis of hydrogel film based on carrageenan extracted from Kappaphycus alvarezii. Mod Appl Sci 7:22
34. Vasconcelos NF, Feitosa JPA, da Gama FMP et al (2017) Bacterial cellulose nanocrystals produced under different hydrolysis conditions: properties and morphological features. Carbohydr Polym 155:425–431
35. Wang LF, Rhim JW (2015) Preparation and application of agar/alginate/collagen ternary blend functional food packaging films. Int J Biol Macromol 80:460–468. https://doi.org/10.1016/j.ijbiomac.2015.07.007
36. Doh H, Whiteside WS (2020) Isolation of cellulose nanocrystals from brown seaweed, Sargassum fluitans, for development of alginate nanocomposite film. Polym Cryst 3:e10133
37. Oun AA, Rhim J-W (2016) Isolation of cellulose nanocrystals from grain straws and their use for the preparation of carboxymethyl cellulose-based nanocomposite films. Carbohydr Polym 150:187–200
38. Kassab Z, Aziz F, Hannache H et al (2019) Improved mechanical properties of k-carrageenan-based nanocomposite films reinforced with cellulose nanocrystals. Int J Biol Macromol 123:1248–1256
39. Yadav M, Chiu F-C (2019) Cellulose nanocrystals reinforced κ-carrageenan based UV resistant transparent bionanocomposite films for sustainable packaging applications. Carbohydr Polym 211:181–194
40. Gaikwad KK, Lee JY, Lee YS (2016) Development of polyvinyl alcohol and apple pomace bio-composite film with antioxidant properties for active food packaging application. J Food Sci Technol 53:1608–1619. https://doi.org/10.1007/S13197-015-2104-9
41. Gaikwad KK, Singh S, Negi YS, Lee YS (2020) The effect of trans-polyisoprene/LDPE based active films on oxidative stability in roasted peanuts. J Food Meas Charact 14:1857–1864. https://doi.org/10.1007/s11694-020-00433-0
42. Kadam AA, Singh S, Gaikwad KK (2021) Chitosan based antioxidant films incorporated with pine needles (Cedrus deodara) extract for active food packaging applications. Food Control 124:107877. https://doi.org/10.1016/J.FOODCONT.2021.107877
43. Kumar A, Gupta V, Singh S, Saini S, Gaikwad KK (2021c) Pine needles lignocellulosic ethylene scavenging paper impregnated with nanozeolite for active packaging applications. Ind Crops Prod 170:113752. https://doi.org/10.1016/j.indcrop.2021.113752
44. Kumar J, Akhila K, Gaikwad KK (2021d) Recent developments in intelligent packaging systems for food processing industry: A review Journal of Food Processing & Technology 12:895
45. Ramakanth D, Singh S, Maji PK, Lee YS, Gaikwad KK (2021) Advanced packaging for distribution and storage of COVID-19 vaccines: a review. Environ Chem Lett 19:3597–3608. https://doi.org/10.1007/s10311-021-01256-1
46. Singh G, Singh S, Kumar B, Gaikwad KK (2021a) Active barrier chitosan films containing gallic acid based oxygen scavenger. J Food Meas Charact 15:585–593. https://doi.org/10.1007/s11694-020-00669-w
47. Singh AK, Ramakanth D, Kumar A, Lee Y. S, Gaikwad KK (2021b) Active packaging technologies for clean label food products: a review. J Food Meas Charact 15:4314-4324. 10.1007/s11694- 021-01024-3
48. Singh S, Maji PK, Lee YS, Gaikwad KK (2021c) Applications of gaseous chlorine dioxide for antimicrobial food packaging: a review. *Environmental Chemistry Letters 19*:253–270. https://doi.org/10.1007/s10311-020-01085-8
49. Tanwar R, Gupta V, Kumar P, Kumar A, Singh S, Gaikwad KK (2021) Development and characterization of PVA-starch incorporated with coconut shell extract and sepiolite clay as an antioxidant film for active food packaging applications. Int J Biol Macromol 185:451–461. https://doi.org/10.1016/j.ijbiomac.2021.06.179